

Effect of Heat Treatment on the Mechanical Properties and Microstructures of Zirconium-Titanium-steel Composite Plate

Zhou Binbin^{1,2}, Ye Cheng³, Zhang Bojun³, Li Jian^{1,2}, Chang Le^{1,2},
Qiu Weiguang^{1,2}, Zhou Changyu^{1,2}

¹ Nanjing Tech University, Nanjing 211816, China; ² Jiangsu Key Lab of Design and Manufacture of Extreme Pressure Equipment, Nanjing 211816, China; ³ Nanjing Boiler and Pressure Vessel Inspection Institute, Nanjing 210028, China

Abstract: In order to obtain better comprehensive performances of Zr/Ti/steel composite plate, the effect of heat treatment on Zr/Ti/steel composite plate was investigated. Based on shear test analysis of titanium-steel interface, the trend has been found that shear strength decreases along with the heat treatment temperature. Besides, the shear strength vertical to wave direction is higher than that parallel to wave direction. Based on orthogonal test and variance analysis, it is found out that the significance of heat treatment on shear strength and bonding strength is that: holding temperature > holding time > temperature change rate. The fracture appearance of shear specimen is ductile fracture including local brittle fracture. The heat treatments of 500 °C, 2 h, 60 °C/h and 540 °C, 1 h, 60 °C/h are both appropriate heat treatment processes through the analysis of microstructure and micro-hardness on interface. With the holding temperature increasing, the grains become coarsening and the brittle intermetallic compounds-FeTi is formed. The micro-hardness of interface drops along with the increase in heat treatment temperature.

Key words: explosive welding; heat treatment; shear strength; bonding strength; microstructure

Explosive welding technology can combine two or more different alloys together. In the process of explosive welding, the energy produced by explosion makes the plate collide at a very high speed, which results in the instantaneous adiabatic fusion of the contact surface^[1,2]. The composite plate made by explosive welding usually combines the advantages of its constituent materials, and even improves its mechanical properties. There have been many studies^[3-8] about explosive welding parameters, welding materials, microstructure and mechanical properties of products. More and more applications of composite plate have been used in chemical and petrochemical industry^[9-14].

Titanium have very good corrosion resistance in face of many mediums, so the titanium/steel composite plate has been widely studied^[15-20]. The corrosion resistance of zirconium is

also excellent, and the corrosion resistances of zirconium and titanium are complementary^[21]. Based on this, Zr/Ti/steel composite plate is produced with Zr as the flyer plate, Ti as the middle plate and steel as the base plate. The interface of the composite plate will show wavy characteristics due to the explosive welding process, and there will be a complex transition zone at the interface, which is not widely understood^[21]. Because of the similarity between Zr and Ti, they are mutually dissolved on the interface in theory^[22]. Therefore, the Ti/steel interface is the focus of studies on Zr/Ti/steel composite plate. Mechanical properties and microstructures of different interfaces of Zr/Ti/steel composite plate have been given in Ref. [22], where composite plate was divided into several parts along the thickness direction to test the mechanical properties. The results showed that there are obvious hardness streng-

Received date: January 25, 2019

Foundation item: National Natural Science Foundation of China (51475223, 51675260); Science-Technology Foundation of Jiangsu Bureau of Quality and Technical Supervision (KJ168359); Postgraduate Research & Practice Innovation Program of Jiangsu Province (KYCX18_1091)

Corresponding author: Zhou Changyu, Ph. D., Professor, School of Mechanical and Power Engineering, Nanjing Tech University, Nanjing 211816, P. R. China, Tel: 0086-25-58139951, E-mail: changyu_zhou@163.com

Copyright © 2020, Northwest Institute for Nonferrous Metal Research. Published by Science Press. All rights reserved.

thening phenomena but slight element diffusion at the interface, and the bending properties of Zr/Ti/steel composite plate can meet the requirements of ASME S264. The microstructures and chemical composition of the interface of titanium/steel composite plate were presented in detail^[21]. It was found that the intermetallic zones at the interface plays the dominant role for the overall mechanical performance of the composite. By test and simulation, the mechanical properties of Ti/steel composite plate and fibrous tissue at the interface were studied, and a detailed analysis of the changes in composition and grain size of the interface were also given by using electron backscattered diffraction (EBSD) technology^[20]. Results showed that the melted zone was dominated by Fe₂Ti intermetallics surrounded by a mixture of FeTi+Fe, and the FeTi intermetallics were observed at Ti/Fe interface.

The heat treatment process was widely used to eliminate the residual stress, which was caused by production process^[23-25]. Proper heat treatment can improve the mechanical properties of the material, while wrong heat treatment will have adverse effects on the materials^[26]. At present, there are few studies about Ti/steel composite plate with different heat treatments. The microstructure of explosively welded titanium (cp-Ti)-stainless steel (AISI 304) with different post-weld heat treatments has been investigated in Ref.[17]. Although the results of the paper were significant, there were few factors of heat treatment to be considered. Therefore, it is necessary to explore the effect of heat treatment on the microstructure and mechanical properties of Zr/Ti/steel composite plate in detail.

In this research, the effects of heat treatment on microstructures, shear and bonding strength of Zr/Ti/steel composite plate were systematically investigated. Scanning electron microscopy (SEM) was used to characterize microstructures of Ti/steel interface.

1 Experiment

The trimetallic composite plate was made up of commercially pure zirconium (Zr702), pure titanium (TA2) and Q345R low alloy steel, where TA2 was used as an interlayer plate to overcome the difficulties of direct explosive welding between Zr702 and Q345R. Fig.1 shows the sketch map of explosive welding. The dimension of formed composite plate was 1500 mm×600 mm×16 mm.

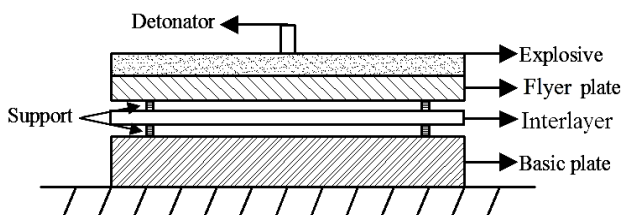


Fig.1 Sketch map for explosive welding

The heat treatment temperature and time range were selected on the basis of relevant researches^[23-27]. The orthogonal test method was used to select sixteen groups of experiments, and the factors and levels were arranged according to L₁₆(4³) orthogonal table. According to different test conditions, heat treatment of Zr/Ti/steel composite plate was carried out one by one, and orthogonal test table was shown in Table 1. Then, the Zr/Ti/steel composite plate was processed into a size of 290 mm×120 mm for heat treatment. In the end, the mechanical tests and microstructure analysis of the Zr/Ti/steel composite plate under different heat treatment conditions were studied.

TA2 was used as the transition layer in Zr/Ti/steel composite plate, so there were two interfaces in this system. Because of the similarity between the properties of Zr702 and TA2, there will be no brittle intermetallic compounds on the bonding surface of Zr/Ti^[22]. Therefore, only the mechanical properties of Ti/steel interface were considered in this research. Fig.2 and Fig.3 show the geometrical dimensions of specimens of shear test and bonding test, and shear strength and bonding strength of Ti/steel interface were measured separately. For each heat treatment, four specimens were tested and their average value was taken. Whether the shear strength was related to the direction of explosion wave was also been considered. The shear tests were divided into two directions: vertical to wave direction and parallel to wave direction. Both shear tests and bonding tests were carried out by a testing machine (MTS-880) at a loading rate of 1.0 mm/min.

Metallographic studies were carried out by using an optical microscope (AXIO Imager A1m). Because the Zr/Ti/steel composite plate was made up of three kinds of alloys, the corrosion resistances of three materials were quite different, which bring difficulties to the preparation of metallographic specimens.

Table 1 Orthogonal test procedure of heat treatment

Test number	Factor		
	T/°C	t/h	v/°C h ⁻¹
1	500	1	30
2	500	2	60
3	500	4	90
4	500	6	120
5	540	1	60
6	540	2	30
7	540	4	120
8	540	6	90
9	580	1	90
10	580	2	120
11	580	4	30
12	580	6	60
13	620	1	120
14	620	2	90
15	620	4	60
16	620	6	30

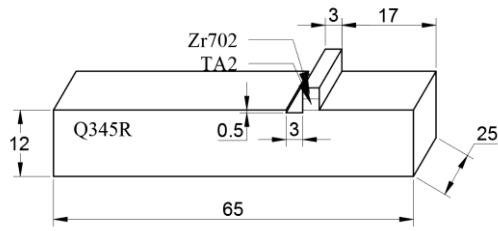


Fig.2 Shear test specimen (mm)

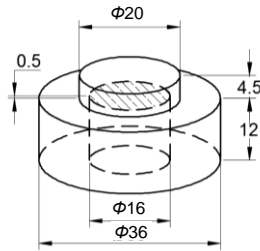


Fig.3 Bonding test specimen (mm)

Table 2 Test results of bonding strength and shear strength of 16 heat treatments (MPa)

Test number	Shear strength		Bonding strength
	Vertical to wave direction	Parallel to wave direction	
1	187.31	189.99	287.18
2	208.28	193.35	283.29
3	198.62	195.31	296.20
4	174.88	168.98	252.19
5	187.98	179.36	314.39
6	164.63	166.97	279.72
7	189.32	170.51	295.97
8	161.10	151.78	266.90
9	161.42	159.92	282.94
10	154.80	150.09	255.71
11	166.08	168.92	251.32
12	153.82	147.59	249.81
13	153.11	153.12	264.41
14	151.14	147.30	229.37
15	153.65	154.26	249.77
16	157.89	159.32	218.78

It was difficult to obtain the microstructures of each alloy by using an erosive agent. Therefore, the stepwise erosion method was used in the metallographic test to corrode the Zr/Ti/steel composite plate. The selection of corrosion reagents was as follows: (1) TA2: kroll reagent (HF:HNO₃:H₂O=3:2:95); (2) Zr702: HNO₃:HF:H₂O=45:20:35; (3) Q345R: nital reagent (4%).

The influence of heat treatment on the fracture mechanism of the composite plates was discussed by using SEM (Phenom ProX).

2 Results and Discussion

2.1 Effect of heat treatment on shear and bonding strength

Table 2 lists the test results of shear and bonding tests of sixteen heat treatments. As shown in Fig.4a, the standard recommended shear strength was drawn by using a dotted line. It was found that the shear strength of two directions of Ti/steel interface decreases with the change of heat treatment process. This was due to the rise of holding temperature and the variation caused by the difference between holding time and temperature change rate. Besides, the shear strength vertical to wave direction is slightly higher than that parallel to wave direction. Because of the differences between positions and materials, the waves of composite plate are not the same everywhere^[5,30]. The error caused by the parameters of wave under the same heat treatment under two directions can be accepted.

As shown in Fig.4b, the bonding strength of Ti/steel interface decreases with the change of heat treatment process. Researchers^[28,29] found that with the increase of holding temperature, the intermetallic compound will increase obviously. The heat treatment process accelerates the diffusion of interfacial elements

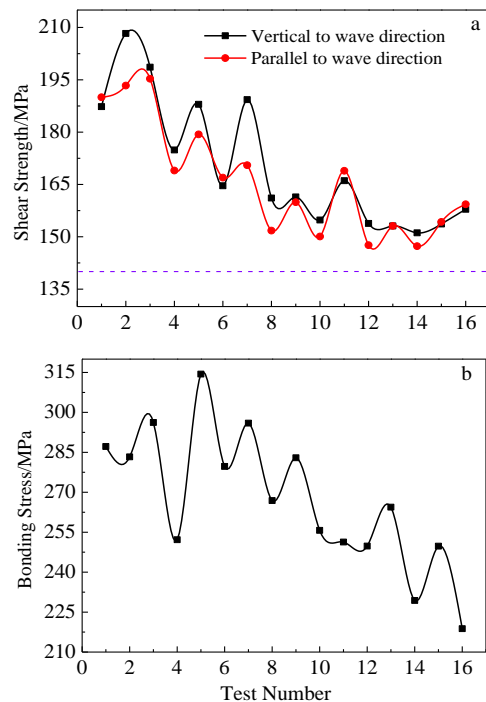


Fig.4 Variation of the shear strength (a) and bonding strength (b)

and the transformation of structure, but weakens the bonding strength. For the heat treatment of Zr/Ti/steel composite plate, its stress annealing temperature cannot be very high, otherwise the bonding strength will be seriously lost. The analysis and prediction of the effect of heat treatment on the bonding properties have been given in detail in previous work^[30].

Fig.5 shows fracture morphology of shear specimen with different shear directions, where the periodic convex and concave trenches can be clearly seen, that is, the wave formed by explosive welding^[18]. The trace of shear force vertical to the direction of wave can be seen from Fig.5a, while the trace of shear force is parallel to the wave direction in Fig.5b and the whole fracture process belongs to the shear slip fracture. Besides, the main fracture morphology of the interface is characterized by slip bands and dimples.

2.2 Variance analysis of shear strength and bonding strength

As shown in Table 3, *ss* is the variance of results, and *P* is a decline index of reliability of the result. The smaller the *P* value is, the more obvious the level of reliability is. It is found that the *ss* of *T* is the biggest, followed by *t*, and that of *v* is smallest. The influence of each factor of heat treatment on shear strength and bonding strength can be both expressed as: $T > t > v$.

2.3 Fracture analysis

2.3.1 Shear test

According to shear strength results in Table 2, the heat treatment condition with maximum shear strength is 500 °C, 2 h, 60 °C/h. Fig.6 shows the fracture morphology of shear test under 500 °C, 2 h, 60 °C/h. It should be noted that Fig.6b, 6c and 6d are enlarged pictures of the b, c and d region in Fig.6a. Fig.6b is the micromorphology of wave peak, it was found that a lot of parallel bars appeared on the surface. This is because when the shear strength is greater than the shear stress of the bonding in-

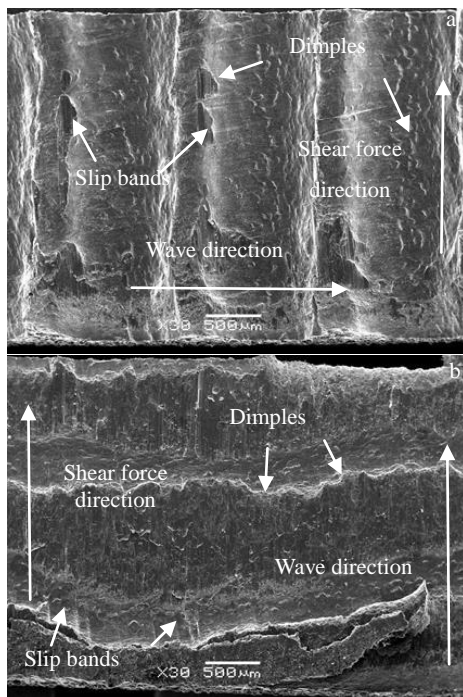


Fig.5 Fracture morphologies of shear specimen: (a) vertical to wave direction and (b) parallel to wave direction

Table 3 Analysis of variance of shear strength

Factor	Shear strength		Bonding strength	
	<i>ss</i>	<i>P</i>	<i>ss</i>	<i>P</i>
<i>T</i>	3140.454	0.005724	5615.655	0.000506
<i>t</i>	520.692	0.211180	3505.885	0.001837
<i>v</i>	163.606	0.617609	465.996	0.154875
Residual	512.856	—	370.272	—

terface, the shear slip friction occurs at the interface, which leads to the interfacial cracking. Besides, it was found that the micro pores in the view were the elongated shear dimples produced by the shear friction. Fig.6c is the transition region of the wave peak and the trough, which is characterized by dense shear dimples, and can be classified as ductile fracture. As shown in Fig.6d, there are obvious cleavage fractures and steps like cleavage fracture surfaces with river patterns of the local characteristic morphology in the transition regions. The morphology is a typical cleavage fracture. Some small pieces of grains and micro cracks are also found in the image, which is due to the great impact force generated in the explosive welding process. Moreover, the broken zone caused by explosive welding process may lead to the fracture in shear test, which indicates that the shearing process has some brittle fracture part.

Based on the above analysis, it was considered that the shear fracture form of the Ti/steel interface is mainly ductile fracture and exhibits brittle fracture in part.

2.3.2 Bonding test

Fig.7 shows the fracture morphologies of bonding test under 540 °C, 1 h, 60 °C/h, where the bonding strength is highest in Table 3. It should be noted that Fig.7b is the enlarged picture of region b in Fig.7a, and Fig.7c and 7d are enlarged images of region c and region d in Fig.7b. The periodic convex and concave grooves can be clearly seen from Fig.7a, where the wave bonding surface is formed by explosive welding^[31].

Fig.7b is the transition pattern of peaks and troughs. As can be seen from Fig.7c, the center of trough has a larger cleavage fracture surface. Steps-like cleavage fracture surface can be seen in the transition region of peak and trough and there is predominant cleavage river pattern on the fracture surface. Besides, it can be seen that the surface of wave peak (titanium side) contains some secondary cracks. In Fig.7d, there are shear dimples with a certain width on the slope between transition of peak and trough. This is due to the consistency of inclined plane with the stress direction applied in the test, resulting in a certain shear stress here and parabolic dimples^[32].

The comprehensive analysis shows that under 540 °C, 1 h, 60 °C/h, the bonding fractures of the composite plate Ti/steel interface are the ductile and cleavage fracture. This is due to the melting, segregation and inclusion in the process of collision, which destroy the continuity of material surface. Fine grained plastic deformation caused by explosive welding makes the material toughness decrease.

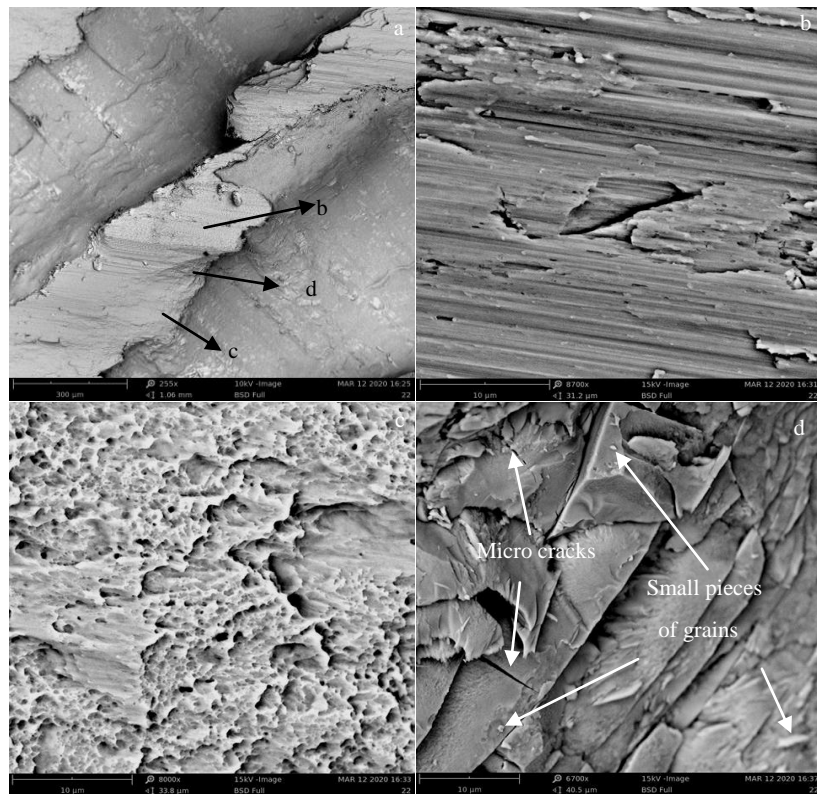


Fig.6 Fracture morphologies of shear test: (a) fracture morphology, (b) the top of the wave, (c) transition area, and (d) local shatter zone morphology

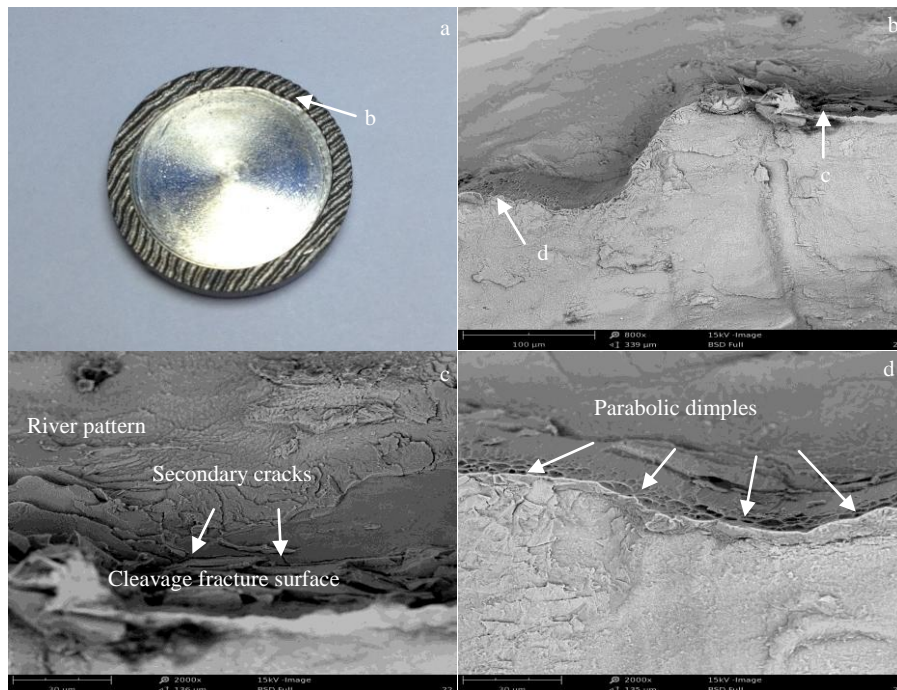


Fig.7 Fracture morphologies of bonding test: (a) macroscopic fracture surface, (b) transition area, (c) trough fracture surface, and (d) crest fracture surface

2.4 Effect of heat treatment on microstructure, element distribution and EDS results

2.4.1 Microstructure of composite plate interface under 500 °C, 2 h, 60 °C/h

The microstructures of three materials under 500 °C, 2 h, 60 °C/h are shown in Fig.8a~8c. From Fig.8a, a small amount of equiaxed α -Zr grains can be seen, but the size is not uniform. The microstructure is not completely recrystallized. As shown in Fig.8b, a small amount of equiaxed α -Ti grains and elongated α -Ti grains can be seen, and the grain size is not uniform, either. The Ti layer is not completely recrystallized by annealing for elimination of stress.

The fine grain zone located in the interface can be observed in the above three images, which is mainly due to the instantaneous adiabatic shear at the collision point between different materials. The jet particles produced by this process are extruded continuously between two plates during the injection process, and it was quickly cooled by the ambient temperature plate. There is not enough time for fine grains in the high temperature melting state to get into recrystallization and the grain growth is cooled and frozen. A layer of fine grain zone is formed^[20]. Tremendous pressure caused by explosion results in

plastic deformation on the interface, thus increasing the dislocation density and lattice distortion. Finally, a thin layer of fine grain zone is formed, which is usually composed of the flow layer and the distortion layer^[26].

2.4.2 Comparison of microstructures under different heat treatment conditions

As shown in Fig.8d~8f, 8g~8i and 8j~8l, microstructures of three other typical heat treatments, 540 °C, 1 h, 60 °C/h; 580 °C, 4h, 30 °C/h and 620 °C, 6 h, 30 °C/h, are also presented.

(1) Zr layer

In Fig.8a, a small amount of equiaxed α -Zr grains are found, and the grains are finely polygon. At this temperature, the grains are not completely recrystallized, and there is a fine grain zone at the interface.

In Fig.8d, equiaxed α -Zr grains are also found, where grain size becomes larger but still not completely crystallized.

As shown in Fig.8g, the recrystallization has been completed and the grains are relatively homogeneous, and a very thin element diffusion layer begins to appear at the Zr/Ti interface.

Fig.8j shows equiaxed α -Zr grains. The grains grow uniformly and obviously. Besides, the fine grain zone at interface disappears and the diffusion layer of Zr/Ti is thickened.

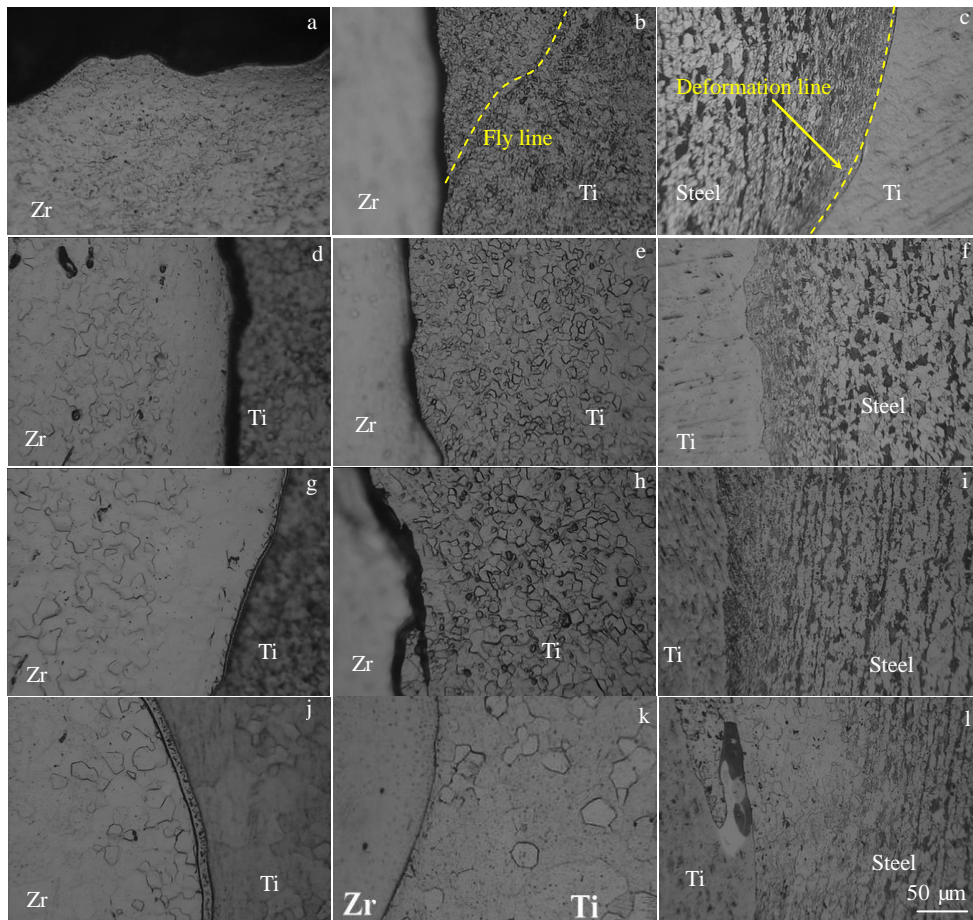


Fig.8 Microstructures of composite plate interface under different heat treatment conditions: (a~c) 500 °C, 2 h, 60 °C/h; (d~f) 540 °C, 1 h, 60 °C/h; (g~i) 580 °C, 4 h, 30 °C/h; (j~l) 620 °C, 6 h, 30 °C/h

(2) Ti layer

In Fig.8b, the microstructures are composed of a small amount of equiaxed α -Ti grains and elongated strips of α -Ti grains, which are annealed with incomplete recrystallization microstructures. There is a fine grain zone at Zr/Ti interface. Besides, there is an obvious fly line structure on the Ti side, which is essentially a plastic deformation line caused by explosive load.

As shown in Fig.8e, partial α -Ti grains are found and the grain size becomes larger and uniform. The fine grain structures at the interface decrease obviously, and the fly line structure observed in Fig.8b disappears.

In Fig.8h and 8k, the microstructures are similar, and the grains have grown obviously, which are equiaxed α -Ti grains.

(3) Steel layer

In Fig.8c, ferrite and pearlite structures are found. The obvious deformation line^[20] is found at Ti/steel interface, where grains are elongated and the deformation is the most serious. With the increase of distance from interface, the deformation is weakened.

As shown in Fig.8e, some pearlite structures decrease, but the deformation line still exists and deformation of elongated grains has been relieved.

Fig.8h shows that pearlite structures continue to decrease, a small amount of deformation lines appear. Besides, there are some black regions and a fine grain zone at the interface. What's more, there is a sign of recrystallization at the interface.

In Fig.8l, the deformed microstructure and black region at the interface disappears, and the deformation line disappears too. The microstructures are composed of the equiaxed ferrite structures and a small amount of fine granular carbides, and the grains grow up. Besides, some pearlite structures are found far away from the interface.

A comprehensive analysis shows that different levels of new grains and recrystallization appear under four heat treatment conditions, and the phenomenon of grain growth has occurred. It is indicated that the residual stress caused by plastic deformation has been eliminated. There are fine grains in 500 °C, 2 h, 60 °C/h and 540 °C, 1 h, 60 °C/h, and no obvious element diffusion zone is found. However, when the heat treatment is 580 °C, 4 h, 30 °C/h or 620 °C, 6 h, 30 °C/h, the grain grows, and the increase of coarse grain and diffusion layer of elements will seriously reduce the strength of interface.

2.4.3 Effect of heat treatment on EDS and microhardness results

The shear fracture analyses of Ti/steel interface under two heat treatment processes, 500 °C, 2 h, 60 °C/h and 620 °C, 6 h, 30 °C/h, were carried out by EDS. It can be observed from Fig.9a and Table 4 that the Fe content of only 6.59% is not enough to form Ti-Fe compounds. When heat treatment process is 620 °C, 6 h, 30 °C/h, Fe content has reached 40.47% and the content of Ti is 56.66%. However, the solubility of Fe in α -Ti is less than 0.1% at 620 °C. Therefore, the Fe-Ti metal compounds

is formed, and the diffusion of element Mn is found. As shown in Fig.9b, the appearance of morphologies of brittle fracture seriously reduces the shear strength of interface. Therefore, it was verified that the severe diffusion of elements caused by excessive holding temperature will produce brittle intermetallic compounds at the interface, which is harmful to the strength of interface.

It can be seen from the Fig.10 that the hardness of the interface is much higher than that of the two sides. The micro hardness of both sides of the interface decreased significantly after heat treatment, and it is found that the micro hardness decreased with the increase of holding temperature and holding time. That is because the morphology of disorderly grains on both sides of composite plate will be improved after heat treatment. Besides, the recovery of plastic deformation zone of material is accompanied by recrystallization, and the dislocation density of grain decreases and the grain grows.

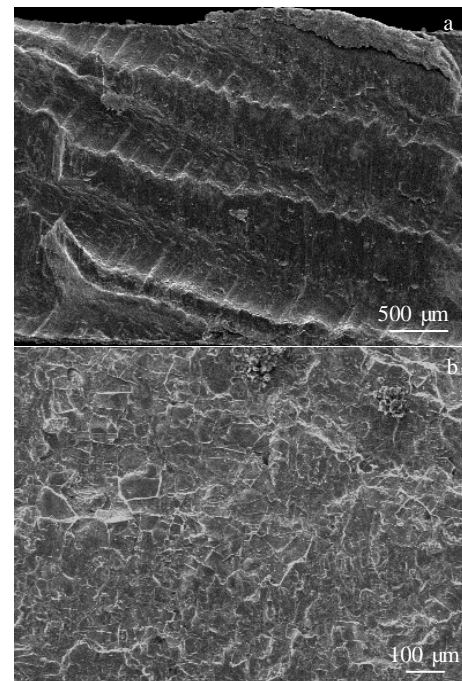


Fig.9 Shear fractures under different heat treatment conditions: (a) 500 °C, 2 h, 60 °C/h and (b) 620 °C, 6 h, 30 °C/h

Table 4 Elements content change of shear fracture

Element	Element content%	
	500 °C, 2 h, 60 °C/h	620 °C, 6 h, 30 °C/h
Ti	93.21	56.66
Fe	6.59	40.47
Al	0.20	0.19
Mn	—	0.94

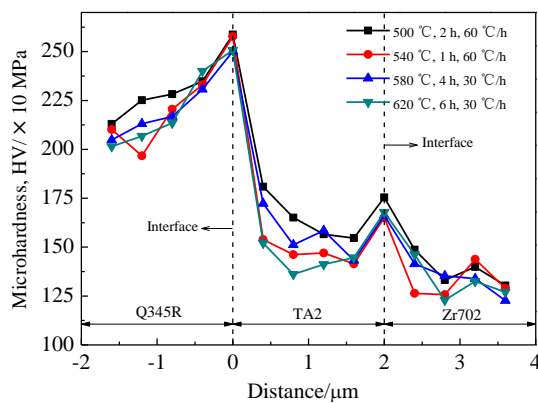


Fig.10 Change trend of microhardness

3 Conclusions

1) Based on orthogonal test and variance analysis, it was found that the significance of heat treatment of shear strength is that: $T > t > v$. Shear strength reaches the maximum value when holding temperature is 500 °C, holding time is 2 h and temperature change rate is 60 °C/h.

2) Based on orthogonal test and variance analysis, the significance of heat treatment of bonding strength is that: $T > t > v$. Bonding strength reaches the maximum value when holding temperature is 540 °C, holding time is 1 h and temperature change rate is 60 °C/h.

3) The fracture appearance of shear test is ductile fracture including local brittle fracture, while the bonding fracture is the ductile and cleavage fracture.

4) The heat treatments of 500 °C, 2 h, 60 °C/h and 540 °C, 1 h, 60 °C/h are both appropriate heat treatment processes through the analysis of microstructure and microhardness on bonding interface.

Reference

- Akbari Mousavi S A A, Al-Hassani S T S. *Materials & Design*[J], 2008, 29(1): 1
- Findik F. *Materials & Design*[J], 2011, 32(3): 1081
- Han J H, Ahn J P, Shin M C. *Journal of Materials Science*[J], 2003, 38(1): 1
- Manikandan P, Hokamoto K, Fujita M et al. *Journal of Materials Processing Technology*[J], 2008, 195(1-3): 232
- Zareie Rajani H R, Akbari Mousavi S A A. *Materials Science and Engineering A*[J], 2012, 556: 454
- Mendes R, Ribeiro J B, Loureiro A. *Materials & Design*[J], 2013, 51: 182
- Hoseini Athar M M, Tolaminejad B. *Materials & Design*[J], 2015, 86: 516
- Loureiro A, Mendes R, Ribeiro J B et al. *Ciência & Tecnologia dos Materiais*[J], 2017, 29(1): 46
- Durgutlu A, Gülenç B, Findik F. *Materials & Design*[J], 2005, 26(6): 497
- Li X, Ma H, Shen Z. *Materials & Design*[J] 2015, 87: 815
- Zhang N, Wang W, Cao X et al. *Materials & Design*[J], 2015, 65: 1100
- Habib M A, Keno H, Uchida R et al. *Journal of Materials Processing Technology*[J], 2015, 217: 310
- Bazarnik P, Adamczyk-Cieślak B, Gałka A et al. *Materials & Design*[J], 2016, 111: 146
- Fronczek D M, Wojewoda-Budka J, Chulist R et al. *Materials & Design*[J], 2016, 91: 80
- Kahraman N, Gülenç B, Findik F. *Journal of Materials Processing Technology*[J], 2005, 169(2): 127
- Akbari Mousavi S A A, Farhadi Sartangi P. *Materials & Design*[J], 2009, 30(3): 459
- Zhang Z, Peng L, Wang J et al. *Procedia Engineering*[J], 2011, 16: 14
- Gloc M, Wachowski M, Plocinski T et al. *Journal of Alloys and Compounds*[J], 2016, 671: 446
- Rozumek D, Marciniak Z. *Procedia Engineering*[J], 2016, 160: 137
- Chu Q, Zhang M, Li J et al. *Materials Science and Engineering A*[J], 2017, 689: 323
- Song J, Kostka A, Veehmayer M et al. *Materials Science and Engineering A*[J], 2011, 528: 2641
- Ning J, Zhang L, Xie M et al. *Journal of Alloys and Compounds*[J], 2017, 698: 835
- Bae D S, Chae Y R, Lee S P et al. *Procedia Engineering*[J], 2011, 10: 996
- Lazurenko D V, Bataev I A, Mali V I et al. *Materials & Design*[J], 2016, 102: 122
- Hedayati O, Korei N, Adeli M et al. *Journal of Alloys and Compounds*[J], 2017, 712: 172
- Prasanthi T N, Sudha R C, Saroja S. *Materials & Design*[J], 2016, 93: 180
- Jiang H, Yan X, Liu J et al. *Transactions of Nonferrous Metals Society of China*[J], 2014, 24(3): 697
- Qiu weiguang, Zhang Bojun, Ye Cheng et al. *Rare Metal Materials and Engineering*[J], 2017, 46(11): 3451 (in Chinese)
- Zhou Binbin, Qiu weiguang, Zhang Bojun et al. *Rare Metal Materials and Engineering*[J], 2018, 47(4): 3451 (in Chinese)
- Borchers C, Lenz M, Deutges M et al. *Materials & Design*[J], 2016, 89: 369
- Carvalho G H S F, Mendes R, Leal R M et al. *Materials & Design*[J], 2017, 122: 172
- Zu Guoyi, Sun Xi, Zhang Jinghua. *Rare Metal Materials and Engineering*[J], 2017, 46(4): 906 (in Chinese)

热处理对锆-钛-钢复合板力学性能及显微组织的影响

周彬彬^{1,2}, 业成³, 张伯君³, 李建^{1,2}, 常乐^{1,2}, 邱伟光^{1,2}, 周昌玉^{1,2}

(1. 南京工业大学, 江苏 南京 211816)

(2. 极端承压装备设计与制造江苏省重点实验室, 江苏 南京 211816)

(3. 南京市锅炉压力容器检验研究院, 江苏 南京 210028)

摘要: 为了获得更好的锆-钛-钢复合板的综合性能, 研究了热处理对锆-钛-钢复合板的影响。通过对锆-钛-钢界面的剪切强度试验分析, 发现剪切强度随热处理温度的降低而减小。垂直于波纹方向的抗剪强度高于平行于波纹方向的抗剪强度。基于正交试验和方法分析, 热处理因素对剪切强度和粘接强度的影响主次关系是: 保温温度 > 保温时间 > 温度变化率。剪切试验的断口形貌为局部脆性断裂的韧性断裂。通过对力学性能、界面组织和显微硬度的分析, 500 °C, 2 h, 60 °C/h; 540 °C, 1 h, 60 °C/h 的热处理均为合适的热处理工艺。随着保温温度的升高, 晶粒变粗, 界面富集元素富集区和扩散区, 形成脆性金属间化合物 FeTi。界面的显微硬度随热处理温度的升高而降低。

关键词: 爆炸焊接; 热处理; 抗剪强度; 结合强度; 显微组织

作者简介: 周彬彬, 男, 1992 年生, 博士生, 南京工业大学, 江苏 南京 211816, 电话: 0086-25-58139951, E-mail: zhou_b@163.com